J. metamorphic Geol., 2000, **18,** 359–374

Cretaceous high-*P* granulites at Milford Sound, New Zealand: metamorphic history and emplacement in a convergent margin setting

G. L. CLARKE, K. A. KLEPEIS* AND N. R. DACZKO
School of Geosciences, The University of Sydney, Sydney, NSW 2006, Australia (geoffc@mail.usyd.edu.au)

ABSTRACT Granulite facies orthogneiss of the Arthur River Complex (ARC) at Milford Sound, western Fiordland records a complex Early Cretaceous magmatic and orogenic history for the Pacific Gondwana margin that culminated in the emplacement and burial of a dioritic batholith, the Western Fiordland Orthogneiss (WFO). Enstatite-bearing mafic to intermediate protoliths of the ARC and WFO intruded the middle to upper crust. The early deformation history of the ARC is preserved in the Pembroke Granulite, where two-pyroxene S1 assemblages that reflect $P < 8$ kbar and $T > 750\,^{\circ}$C were only patchily recrystallized during later deformation. S1 is cut by garnet-bearing, leucogabbroic to dioritic veins, which are cut by distinctive D2 fractures involving anorthositic veins and garnet–diopside–plagioclase-bearing reaction zones. These zones are widespread in the ARC and WFO and record conditions of $P \approx 14$ kbar and $T > 750\,^{\circ}$C. Garnet–clinopyroxene-bearing corona reaction textures that mantle enstatite in both the ARC and WFO reflect Early Cretaceous burial by approximately 25 km of continental crust. Most of the ARC is formed from the Milford and Harrison Gneisses, which contain steeply dipping S4 assemblages that envelop the Pembroke Granulite and involve garnet, hornblende, diopside, clinozoisite, rutile and plagioclase, with or without kyanite. The *P–T* history of rocks in western Fiordland reflects pronounced Early Cretaceous convergence-related tectonism and burial, possibly related to the collision and accretion of island arc material onto the Pacific Gondwana margin.

Key words: Cretaceous; Fiordland; high-*P* granulite facies; *P–T* path; thermobarometry.

INTRODUCTION

Although granulite facies rocks are common in Precambrian shields, the tectonic settings responsible for their formation are commonly ill-defined, and interpretations of the tectonic significance of metamorphic and deformation events may be equivocal. For granulites that experienced polyphase deformation, most textural information reflects peak and post-peak events (Harley, 1989), due to the intensity of progressive recrystallization at elevated temperature. Most data that could constrain the prograde path experienced by the rocks have been destroyed (Harley, 1989; Greenfield *et al*., 1998). Evidence for *P–T* paths experienced by such terranes is thus commonly limited to peak and post-peak assemblages involving corona reaction textures (McLelland & Whitney, 1977; Clarke & Powell, 1991) or those defining cross-cutting shear zones that may or may not have been causally related to the high-grade events (Austrheim & Griffin, 1985; White & Clarke, 1997).

Western Fiordland, New Zealand, contains one of the most extensive belts of comparatively young high-*P* garnet granulites, and potentially provides an ideal setting to test models for processes that form high-*P* granulite facies conditions in the crust. The rocks of western Fiordland are a composite of Palaeozoic (Ireland & Gibson, 1998) to Early Cretaceous (Mattinson *et al*., 1986) orthogneiss, lesser paragneiss, and an Early Cretaceous batholith referred to as the Western Fiordland Orthogneiss (Oliver, 1980; Bradshaw, 1985, 1990; Fig. 1). In northern Fiordland, granulite facies orthogneisses of the Arthur River Complex (Bradshaw, 1990) are in fault contact (Koons, 1978; Bradshaw, 1985) or show a gradational boundary (Blattner, 1991) with Late Jurassic to Early Cretaceous (*c*. 147–137 Ma) gabbronorite and leucogabbro of the Darran Complex, named after the Darran Diorite (Wood, 1962; Bradshaw, 1990; Kimbrough *et al*., 1994). The Darran Complex is part of a zone of disrupted Early Triassic to Early Cretaceous, subduction-related I-type plutonic rocks and lesser volcanic and sedimentary rocks of the Median Tectonic Zone (Kimbrough *et al*., 1993) that represent relics of a Mesozoic magmatic arc. To the west of the Arthur River Complex are amphibolite facies, Palaeozoic metasediments and orthogneiss that represent the rifted relics of a Triassic to Early Cretaceous Pacific Gondwana margin (Mortimer, 1995; Ireland & Gibson, 1998). Recent investigations have proposed conflicting interpretations for the evolution of parts of western

*Current address: Department of Geology, The University of Vermont, Burlington, VT 05405, USA

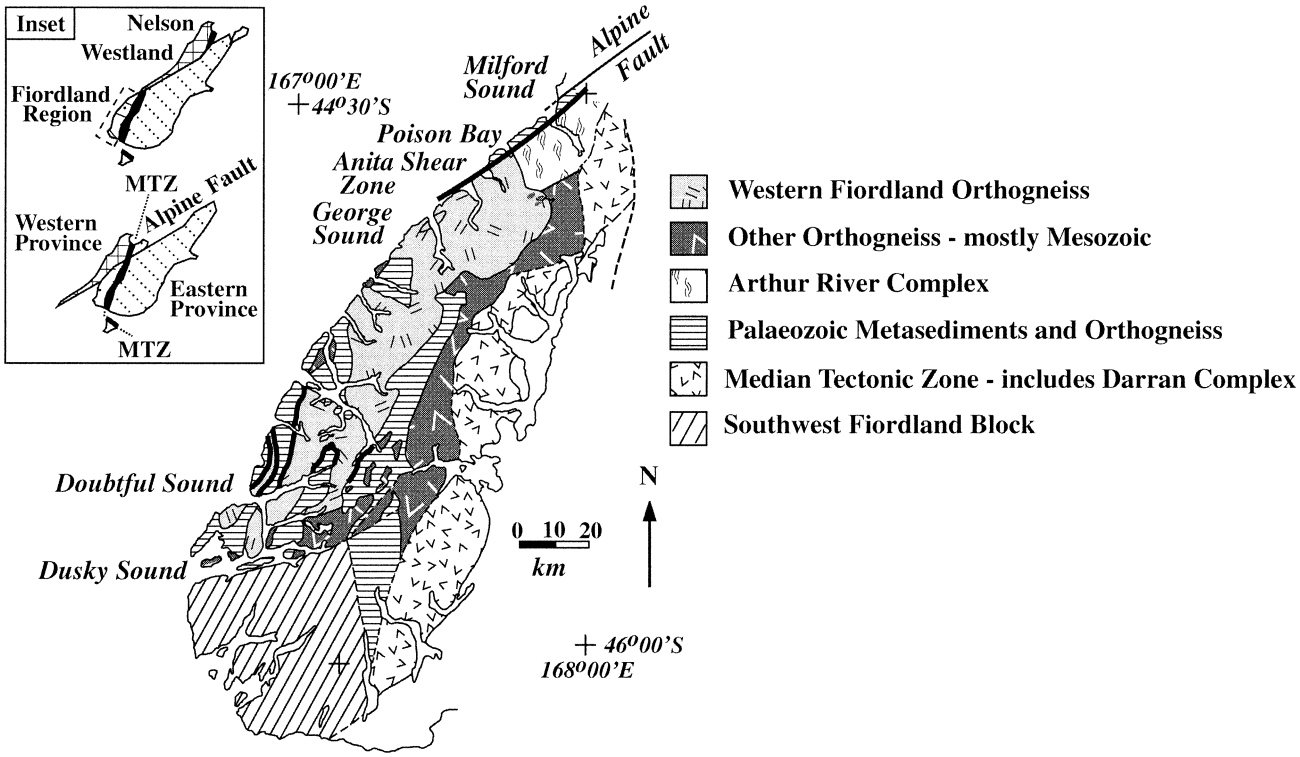

Fig. 1. Geological map of Fiordland showing major lithological divisions (after Bradshaw, 1990). The inset shows pre-Cenozoic configuration of the South Island which places the Westland/Nelson region adjacent to northern Fiordland.

Fiordland, and relationships between the high-grade rocks, the Mesozoic arc and the Pacific Gondwana margin. Mortimer *et al.* (1999) inferred that much of the Median Tectonic Zone intruded into and/or alongside the Pacific Gondwana margin. In contrast, Muir *et al.* (1998) presented geochemical data from which they inferred that part of an allochthonous early Cretaceous magmatic arc, chemically equivalent to rocks of the Darran Complex (Fig. 2), was thrust beneath western Fiordland and melted to produce the Western Fiordland Orthogneiss. Although high-*P* granulite facies metamorphism was broadly contemporaneous with emplacement of the Western Fiordland Orthogneiss at 126–119 Ma (Mattinson *et al.*, 1986; Kimbrough *et al.*, 1994), there is disagreement as to whether mineral assemblages in key areas reflect Palaeozoic or Mesozoic events (Bradshaw, 1985; Gibson *et al.*, 1988). From regional mapping, petrological and geochronological studies, Bradshaw (1989a) and Brown (1996) inferred that most of the high-*P* assemblages are Cretaceous. On the basis of U–Pb dating of zircon, Ireland & Gibson (1998) inferred that recrystallization during the Cretaceous was mostly restricted to contact metamorphic effects related to emplacement of the Western Fiordland Orthogneiss, amphibolite facies shear zones, and limited recrystallization elsewhere. Models involving crustal extension (Gibson, 1990; Gibson & Ireland, 1995), crustal thickening during arc collision (Bradshaw, 1985; Muir *et al.*, 1998) and *in situ* magmatic over-accretion (Brown, 1996; Mortimer *et al.*, 1999) have been proposed for the Mesozoic metamorphism in western Fiordland.

In this paper, we present data to constrain models for the structural and *P–T* history of the Arthur River Complex (Bradshaw, 1990), which includes the northeasternmost exposures of high-grade rocks in Fiordland and lies at the boundary between late Jurassic/Early Cretaceous arc rocks and the inferred Pacific Gondwana margin (Fig. 2). Data from field relationships, thermobarometry and calculated phase diagrams are integrated to define a dynamic Early Cretaceous history. We show that igneous protoliths of both the Arthur River Complex and Western Fiordland Orthogneiss were emplaced in the mid-crust, before experiencing Early Cretaceous burial by more than 20 km of continental crust. The high-*P* granulite facies conditions were attained in a convergent margin setting, possibly when parts of the Median Tectonic Zone were thrust underneath the Pacific Gondwana margin. The exhumation history of the Arthur River Complex is discussed elsewhere (Klepeis *et al.*, 1999).

REGIONAL GEOLOGY

The geology of New Zealand's South Island may be divided into three provinces, which are mostly separ-

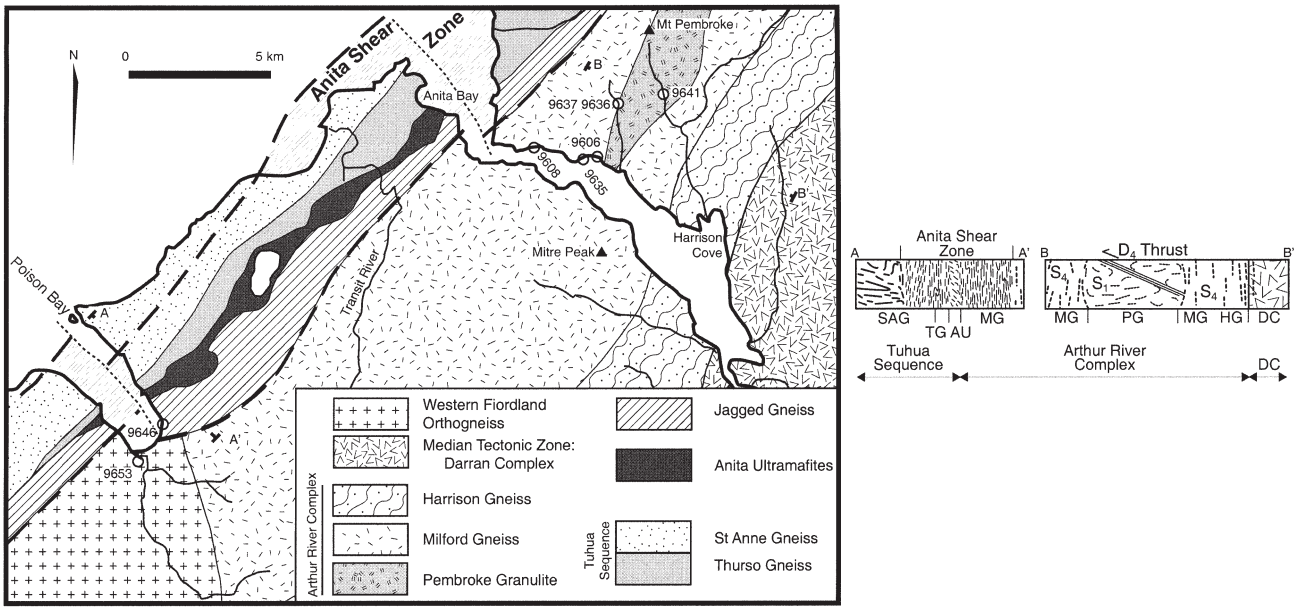

Fig. 2. Geological map of the area between Milford Sound and Poison Bay (after Wood, 1972; Blattner, 1991; Hill, 1995a).

ated by faults (Fig. 1). Mesozoic subduction-related I-type plutonic, volcanic and sedimentary rocks form the Median Tectonic Zone (Kimbrough *et al*., 1993), which is also called the Median Batholith (Mortimer *et al*., 1999). These rocks, together with a series of fault-bound Permian to Early Cretaceous tectonostratographic terranes that form the Eastern Province (Bishop *et al*., 1985), were accreted to Palaeozoic to Cretaceous rocks of the Western Province, which represent a rifted and tectonically dismembered Gondwana margin. U–Pb zircon ages for rocks of the Median Tectonic Zone fall into two age groups: 247–195 and 157–131 Ma (Kimbrough *et al*., 1994). Sedimentary rocks that dominate Eastern Province terranes may have been derived from a long-lived peri-Gondwana Mesozoic magmatic arc, now mostly preserved as plutons of the Median Tectonic Zone (Mortimer, 1995). Late Triassic Median Tectonic Zone plutons that intrude the Eastern Province indicate that these two provinces were together at this time (Williams & Harper, 1978; Mortimer *et al*., 1999). Rocks of the Western Province and the Median Tectonic Zone were intruded by plutons of the 126–105 Ma Western Fiordland Orthogneiss/Separation Point Suite (Kimbrough *et al*., 1994; Fig. 1).

Sparsely dated amphibolite to granulite facies gneisses and schists in western Fiordland record orogeny and magmatism from the Early Palaeozoic to the Mesozoic. It is unclear what proportion of the high-grade rocks are deformed parts of the Median Tectonic Zone (Muir *et al*., 1998) or re-deformed and re-metamorphosed Palaeozoic metasediments and orthogneiss (Ireland & Gibson, 1998). Amphibolite facies metasedimentary schist and orthogneiss (Fig. 2) in northern Fiordland, which are correlated with the Tuhua Sequence (Carter *et al*., 1974), have been divided into the St Anne Gneiss and Thurso Formation (Wood, 1962; Bradshaw, 1990; Fig. 2). They are in fault contact with the Anita Ultramafites (unknown age) and granulite facies orthogneiss of the Arthur River Complex (Wood, 1962, 1972; Bradshaw, 1990). The 126–119 Ma Western Fiordland Orthogneiss (Mattinson *et al*., 1986; Gibson & Ireland, 1995; Figs 1 & 2) is a metamorphosed and variably deformed intrusive complex, characterized by pyroxene-bearing diorite and monzodiorite. The Western Fiordland Orthogneiss intrudes the Arthur River Complex, metasediment and granitoids of uncertain age (Bradshaw, 1990).

The Arthur River Complex of Bradshaw (1990) includes the homogeneous, mafic Milford Gneiss and the compositionally banded, dioritic Harrison Gneiss (Wood, 1972; Blattner, 1991; Fig. 2). Two-pyroxene–hornblende-bearing mafic granofels of the Pembroke Granulite (Fig. 2) occur as a low-strain zone in the Milford Gneiss (Blattner, 1991; see below). The Harrison Gneiss has a faulted (Koons, 1978; Bradshaw, 1985) or gradational (Blattner, 1991) eastern boundary with weakly deformed and weakly metamorphosed leucogabbroic to dioritic plutons of the 137^{+4}_{-1} Ma Darran Complex, in the Median Tectonic Zone (Kimbrough *et al*., 1994). Alhough the Arthur River Complex is commonly placed within the Western Province, whole-rock chemical similarities between the Pembroke Granulite, Milford Gneiss and Darran Complex are consistent with parts of the Arthur River Complex representing deformed and metamorphosed rocks of the Darran Complex (Blattner, 1991). The western boundary of the Arthur River Complex in Milford Sound is marked by a broad zone of mylonite,

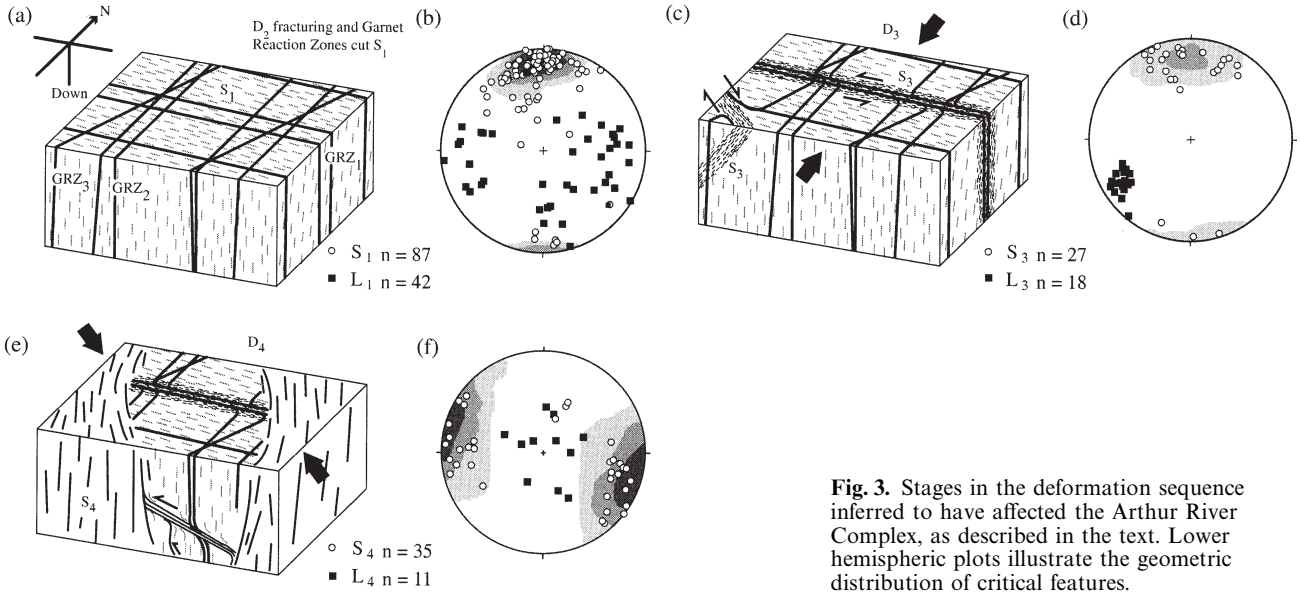

Fig. 3. Stages in the deformation sequence inferred to have affected the Arthur River Complex, as described in the text. Lower hemispheric plots illustrate the geometric distribution of critical features.

protomylonite and cataclasite, which is collectively termed the Anita Shear Zone (Hill, 1995a, 1995b; Fig. 2). Amphibolite to greenschist facies structures in the Anita Shear Zone cut the high-grade assemblages in the Arthur River Complex (Hill, 1995a, 1995b; Klepeis *et al*., 1999). U–Pb analyses of titanite from amphibolite facies assemblages in the shear zone yield mid-Cretaceous and younger ages (K. A. Klepeis & N. R. Daczko, unpublished data).

ARTHUR RIVER COMPLEX: STRUCTURE AND FIELD RELATIONSHIPS

Four deformation/metamorphic events (D1–D4) affected orthogneiss of the Arthur River Complex in the Milford Sound area (after Hollis, 1996; Daczko, 1997; Turner, 1998). The deformation sequence is summarized in Fig. 3.

D1 resulted in a gneissic foliation (S1) in the Pembroke Granulite (Blattner, 1991), defined by hornblende–granulite facies assemblages (Blattner, 1976). S1 is cut by igneous veins and dykes of leucogabbroic to dioritic composition, which may or may not contain large (1–3 cm diameter) euhedral garnet grains. These veins and dykes are commonly 30–100 cm across, and are in turn cut by D2 fractures that are commonly filled with anorthosite. The anorthosite veins are commonly approximately 1 cm in width and acted as the loci for planar garnet-bearing reaction zones (GRZ; Bradshaw, 1989b) in which hornblende was statically pseudomorphed by garnet–clinopyroxene-bearing assemblages (Fig. 4a; Bradshaw, 1989b).

In the Pembroke Valley (Fig. 2), D3 produced east-trending, steeply dipping mylonites that cut S1 and the D2 garnet-bearing reaction zones (Fig. 4b,c). These shear zones contain a shallowly west-plunging mineral and stretching lineation and evidence for sinistral displacement. D3 shear zones are cut by shallowly dipping D4 thrust zones that contain a south-plunging mineral lineation, which locally branches into steeply dipping, anastomosing shear zones. The boundaries of the Pembroke Granulite are not well exposed. However, the orientation of the foliation and lineation in steeply dipping D4 shear zones is identical to the pervasive foliation and lineation in the Milford and Harrison Gneiss, and the two fabrics are inferred by us to be equivalent. In Poison Bay (Fig. 1), the penetrative effects of D4 can be recognized in exposures of the Milford Gneiss and Western Fiordland Orthogneiss (Fig. 2). Here, the western boundary of the Western Fiordland Orthogneiss is defined by the Anita Shear Zone and the eastern boundary is obscured. D4 shear zones are cut by muscovite-biotite-bearing pegmatites, which are deformed by mesoscopic folds that have a steeply dipping, north-east-trending axial plane and are inferred by us to be related to late movement on the Anita Shear Zone. The pegmatites are cut by narrow shear zones that record a mixture of brittle and ductile behaviour and have minor

Fig. 4. (a) Dioritic vein (DV) that cuts S1 in the Pembroke Granulite, and is cut by narrow anorthositic veins and garnet reaction zones (GRZ). Where the garnet reaction zone cuts the diorite vein, igneous hornblende is pseudomorphed by garnet, clinopyroxene and rutile (arrowed). (b) Rectilinear pattern of garnet reaction zones (GRZ), most of which are centred on narrow anorthositic veins. The zones are all steeply dipping. (c) D3 mylonite zones in the Pembroke Granulite, cut by north-trending brittle faults. (d) Coarse-grained leucogabbroic gneiss bodies transposed into S4 in the Milford Gneiss. The base of photograph is approximately 5 m across.

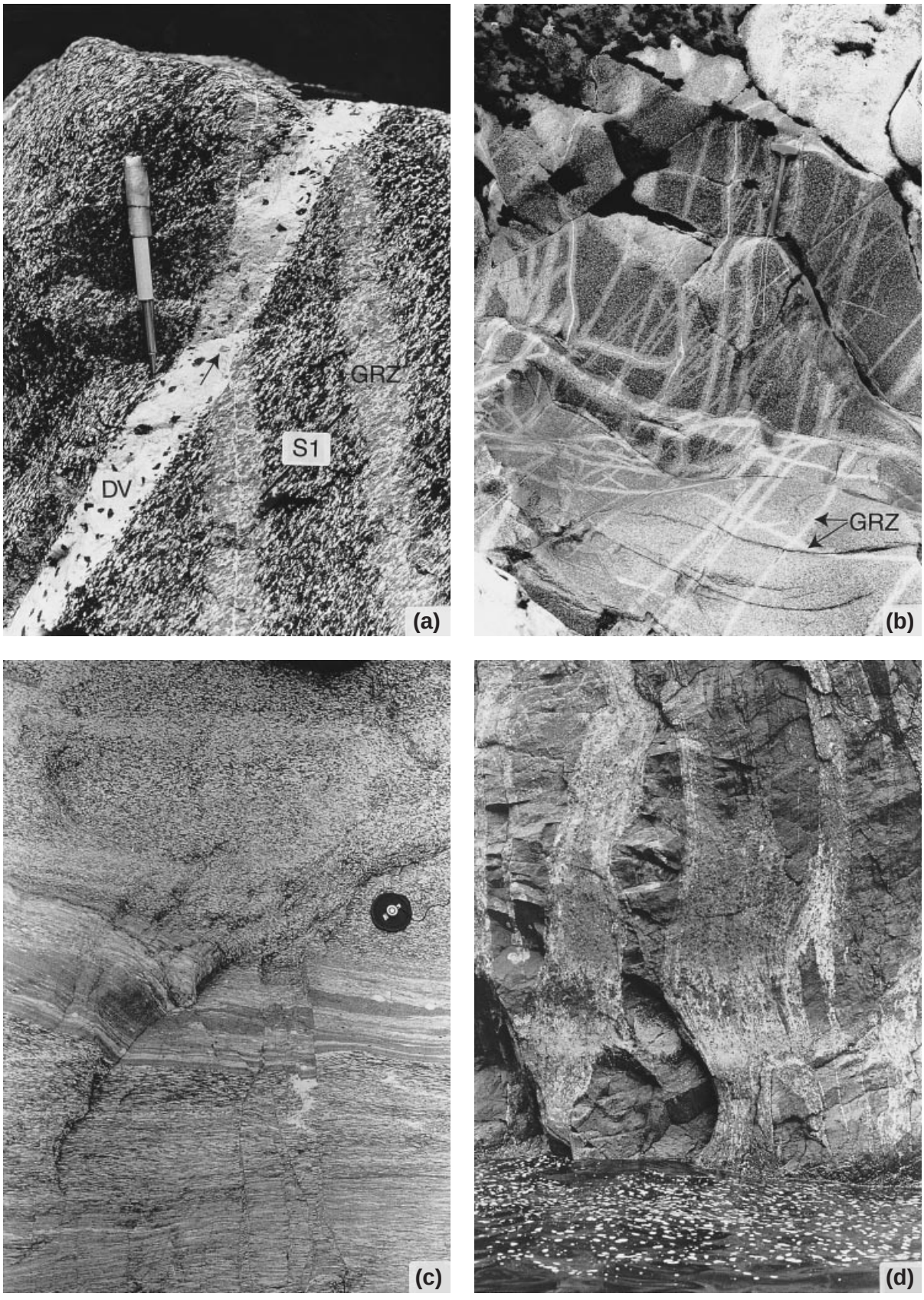
GRZ
S1
DV
(a)
GRZ
(b)
(c)
(d)

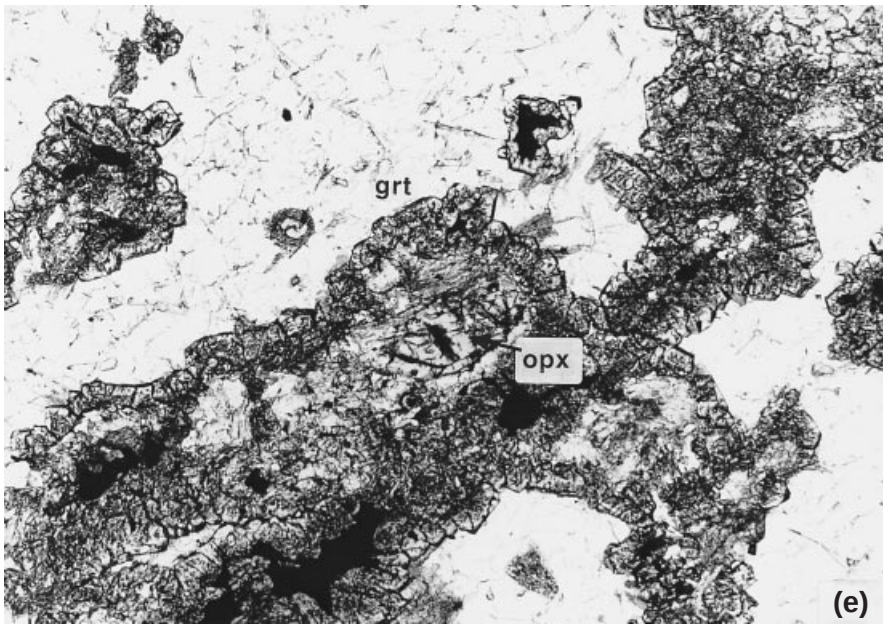

Fig. 4. *Cont'd*. (e) S1 orthopyroxene enclosed by random symplectic intergrowth of clinopyroxene, clinzoisite, biotite and rutile, which is enclosed by a corona of garnet. Random acicular clinozoisite and kyanite occur in plagioclase in the clear matrix. Garnet reaction zone sample 9643b. Plane-polarized light; base of photograph is 3.5 mm.

pseudotachylite. The mylonites contain epidote and chlorite that pseudomorph older ferromagnesian minerals.

PETROLOGY

In this section, we describe the petrology of orthogneiss exposed at Milford Sound and Poison Bay, concentrating on assemblages that are useful in constraining the metamorphic history.

Arthur River Complex

Pembroke granulite

In the Pembroke Valley (Fig. 2), the Pembroke Granulite is dominantly gabbroic, but ultramafic and dioritic compositions occur both as discontinuous pods in gabbroic gneiss and as larger units covering hundreds of square metres. Boundaries between these compositions are sharp, and, on the basis of igneous textures preserved in low-strain domains, are inferred to be igneous. In gabbroic rocks, igneous clinopyroxene occurs as euhedral grains 3–10 mm in length. Igneous orthopyroxene is finer-grained, grains being 1–3 mm in length, and commonly occurs as inclusions in igneous clinopyroxene. Igneous pyroxene grains contain fine-grained (10 μm in length) ilmenite and hematite exsolution lamellae. Areas with igneous textures are enveloped by high-strain domains containing S1 minerals that preserve flaser textures and include deformed grains up to 10 mm in length. Rocks pervasively recrystallized during D1 have the assemblage hornblende (*c*. 40%), clinopyroxene (10%), plagioclase (35%), ilmenite (1%), quartz (2%) and apatite (1%), with or without orthopyroxene (5%) and biotite (1%). Proportions of the minerals were obtained by point counting.

Most ultramafic bodies in the Pembroke Valley were extensively recrystallized during D1 to amphibolite that contains S1 hornblende, clinopyroxene, plagioclase, quartz, apatite and ilmenite. In most rocks, it is difficult to clearly distinguish the effects of recrystallization during later deformation; pods may also contain clinozoisite, rutile and garnet that are inferred to have grown during D3 and D4. An ultramafic pod in the Milford Gneiss, on the north shore of Milford Sound (Fig. 2), contains ophitic textures defined by coarse-grained olivine, plagioclase, clinopyroxene, orthopyroxene and ilmenite. This ultramafic body is enveloped by a penetrative S4 foliation in the Milford Gneiss; the timing of emplacement with respect to S1 is unclear.

Post-S1 igneous veins

S1 is cut by pegmatitic leucogabbroic to dioritic veins and dykes. The veins vary from a few centimetres to two metres in width, and contain euhedral grains of hornblende, clinopyroxene, plagioclase and garnet, with or without anhedral quartz, ilmenite, rutile and scapolite. Scapolite occurs as inclusions in garnet, and clinopyroxene is intergrown with garnet. Garnet is spread irregularly through the veins as large euhedral grains. These veins are cut by narrow D2 fractures that are filled by pegmatitic to aplitic anorthosite, which form a lattice-like network in the Pembroke

Granulite (Blattner, 1976; Fig. 4b). Garnet defines selvages on one or both margins of these anorthositic veins, or forms a thick central septum to veins in dioritic hosts. Euhedral habit and composition distinguish garnet in these igneous veins from garnet in the reaction zones, as discussed below.

Garnet reaction zones

Domains of bleached country rock are common on the margins of the post-S1 anorthositic veins and may extend up to 100 mm into the surrounding gabbroic gneiss. These garnet reaction zones form rectilinear fracture networks in domains of low D3 and low D4 strain (Blattner, 1976; Fig. 4b). The deformed equivalents of these garnet reaction zones can be recognized through much of the Milford Gneiss, but are best exposed in the Pembroke Valley (Fig. 2). In individual garnet reaction zones, the proportion of clinopyroxene increases, and the proportion of hornblende decreases, as the felsic veins are approached. Layered corona reaction textures are preserved locally within the garnet reaction zones, involving garnet and clinopyroxene assemblages armouring orthopyroxene and hornblende (Fig. 4e). Hornblende, orthopyroxene and plagioclase from igneous and S1 assemblages are partially to completely pseudomorphed (Blattner, 1976; Blattner & Black, 1980; Bradshaw, 1989b) by assemblages involving garnet (*c.* 30–40%), clinopyroxene (10–20%), plagioclase (30–50%), clinozoisite (5%), quartz (2–4%) and rutile (2%), with or without scapolite (1%), K-feldspar (< 1%) and kyanite (1–2%). On the basis of element mapping using an electron microprobe, igneous and S1 plagioclase is patchily recrystallized to fine-grained intergrowths of less calcic plagioclase and K-feldspar. Kyanite and clinozoisite are mostly hosted by plagioclase, but may occur adjacent to garnet and clinopyroxene. Where post-S1 hornblende diorite veins are cut by the garnet reaction zones, hornblende phenocrysts are partially to completely pseudomorphed by garnet, clinopyroxene and rutile. Large garnet grains in these post-S1 diorite veins commonly have a rim that is compositionally distinct from the core, the rim garnet composition being similar to that of garnet in the reaction zone. Where cut by D3 and D4 mylonites, garnet reaction zone assemblages are recrystallized to S3 and S4 assemblages of garnet, hornblende, clinopyroxene, clinozoisite, plagioclase, quartz and rutile.

Milford Gneiss

D4 resulted in a penetrative gneissic foliation (S4) in the hornblende-rich Milford Gneiss. The foliation is locally protomylonitic and the intensity of, and mineral assemblage defining, S4 varies. In low-strain domains, deformed GRZ can be recognized, and garnet and clinopyroxene define S4. In most places, S4 is defined by aligned hornblende, plagioclase, clinozoisite, phengitic white mica and rutile, with or without garnet, clinopyroxene and biotite. The grains are commonly 1–4 mm across, and evidence for the earlier structures was mostly destroyed by the intensity of recrystallization. The S4 assemblage—hornblende, plagioclase, clinozoisite, margarite, kyanite, rutile, garnet, clinopyroxene and biotite—is also observed (sample 9606). Sheets of diorite and coarse-grained leucogabbro that are correlated with the post-S1 igneous veins in the Pembroke Granulite were transposed into S4 in the Milford Gneiss (Fig. 4d). Large grains (10–20 mm across) of diopside, garnet, plagioclase, hornblende, quartz, clinozoisite, rutile and quartz define S4 in the leucogabbro. They are enveloped by mylonitic S4 folia that contain identical, but finer-grained assemblages.

Harrison Gneiss

The dominant mineral assemblage in the Harrison Gneiss involves hornblende, plagioclase and clinozoisite, with or without scapolite, garnet, biotite and phengitic white mica. Hornblende, plagioclase and clinozoisite define a penetrative gneissic foliation (S4), which is locally intra-folially folded. A pronounced compositional banding is defined by alternating, discontinuous mafic and felsic layers. The mafic layers tend to be comparatively thin (150–600 mm thick) and have S4 assemblages similar to those described above for the Milford Gneiss near the Pembroke Granulite (Fig. 2), but with less garnet. The felsic bands are comparatively thick (up to several metres wide), and have S4 assemblages dominated by plagioclase, quartz and hornblende.

Darran Complex

Leucogabbro, diorite and monzonite of the Darran Complex (Fig. 1) mostly preserve igneous assemblages. Ophitic textures are defined by large clinopyroxene and orthopyroxene phenocrysts (up to 100 mm length), hornblende, plagioclase, ilmenite and biotite. Limited effects of metamorphism can be recognized in a narrow transition zone near the contact with the Arthur River Complex. In Harrison Cove (Fig. 2), the transition zone is a few hundred metres wide and contains domains with ophitic textures enveloped by proto-mylonitic amphibolites. In these proto-mylonitic zones, coarse-grained (5–10 mm) hornblende, clinozoisite, rutile, plagioclase and quartz define a foliation co-planar with S4 in the Arthur River Complex (Hollis, 1996). White mica may extensively pseudomorph plagioclase. Garnet occurs in felsic domains as symplectic intergrowths with plagioclase, quartz, ilmenite and rutile. To the north of Milford Sound, the contact between the Arthur River Complex and the Darran Complex is defined by the Kaipo Fault (Blattner, 1976).

Western Fiordland Orthogneiss

Exposures of lightly coloured Western Fiordland Orthogneiss occur east of the Anita Shear Zone in Poison Bay (Fig. 2). The Western Fiordland Orthogneiss contains two-pyroxene igneous assemblages that were partially recrystallized during high-grade metamorphism. The exposures do not contain a penetrative high-grade foliation, making it difficult to relate the recrystallization to the structural scheme developed for the Arthur River Complex. Orthopyroxene and some clinopyroxene grains are clouded by fine-grained exsolution lamellae of ilmenite, and are inferred by us to be igneous. Igneous orthopyroxene, with or without igneous clinopyroxene, is separated from plagioclase, quartz and K-feldspar by metamorphic aggregates of clinopyroxene, garnet and rutile. These aggregates may have a weak to well-developed structure involving a small core of igneous orthopyroxene or clinopyroxene, successively mantled by metamorphic clinopyroxene and garnet. Small proportions of hornblende occur intergrown with metamorphic clinoyroxene near the margins of the aggregates. Quartz, K-feldspar, plagioclase, rutile and the garnet and clinopyroxene aggregates define a weak foliation. Within and adjacent to steeply dipping high-strain zones of the Anita Shear Zone, the rock becomes a much darker, well-lineated, hornblende-dominated schist—the Jagged Gneiss of Bradshaw (1990).

MINERAL CHEMISTRY

Below we outline the major features of mineral chemistry in rocks that are important in constraining their metamorphic evolution in the Milford Sound area. Representative microprobe analyses of minerals from some critical rock types are given in Table 1.

Igneous *clinopyroxene* in gabbroic parts of the Pembroke Granulite has X_{Fe} [Fe/(Fe + Mg)] = 0.29–0.37. When recalculated using the method of Cawthorn & Collerson (1974), it has the general formula $Di_{58}Hed_{24}Ens_9Fs_4Ca\text{-}tsch_5$. The igneous clinopyroxene grains show a subtle rimward decrease in Mg and Ca content, and an increase in Al and Na content. S1 clinopyroxene has X_{Fe} 0.31–0.37, and has the general formula $Di_{47}Hed_{24}Ens_3Fs_2Ca\text{-}tsch_{11}$. Clinopyroxene in GRZ has X_{Fe} 0.17–0.29 and the general formula $Di_{58}Hed_{20}Jd_{12}$. S4 clinopyroxene grains in the Milford Gneiss are compositionally similar to clinopyroxene in D3 and D4 mylonite zones in the Pembroke Granulite. They have X_{Fe} 0.17–0.28 and the general formula $Di_{56}Hed_{20}Jd_{12}Ca\text{-}tsch_9Aeg_3$. Igneous clinopyroxene in the Western Fiordland Orthogneiss at Poison Bay has the general formula $Di_{41}Hed_{21}Ens_{11}Fs_6Ca\text{-}tsch_{14}$, whereas the metamorphic clinopyroxene has the general formula $Di_{46}Hed_{20}Jd_{12}Ca\text{-}tsch_9$.

Igneous *orthopyroxene* in gabbroic parts of the Pembroke Granulite has X_{Fe} 0.43–0.47; the composition of S1 orthopyroxene is identical. Igneous orthopyroxene in the Western Fiordland Orthogneiss at Poison Bay has X_{Fe} *c.* 0.34, with approximately 8% Mg-tschermakite component. Igneous *plagioclase* in the Pembroke Granulite is andesine, with X_{An} [Ca/(Ca + Na)] = 0.32–0.47. Metamorphic plagioclase mostly straddles the oligoclase/andesine boundary: X_{An} = 0.25–0.39 in the Pembroke Granulite, 0.28–0.32 in GRZ and the Milford Gneiss, and 0.29–0.32 in the Western Fiordland Orthogneiss. *K-feldspar* in the Western Fiordland Orthogneiss has X_{or} [K/(K + Na)] = 0.92. S1 *amphibole* in the Pembroke Granulite and Western Fiordland Orthogneiss is pargasite (after Leake, 1978). The composition of amphibole in the rocks varies with textural setting. Hornblende that forms rims on igneous ilmenite is richer in Fe, Ti and Si, and poorer in Na, K and Al than hornblende that forms rims on pyroxene. S3 and S4 amphibole in the Milford Gneiss is pargasitic hornblende that shows a wide range of composition, with X_{Fe} 0.26–0.46.

Large *garnet* grains from post-S1 diorite veins in the Pembroke Granulite are mostly unzoned pyrope-rich almandine with $Alm_{50}Spss_3Py_{31}Gr_{16}$ where Alm = 100 Fe/(Fe + Mg + Mn + Ca), Spss = 100 Mn/(Fe + Mg + Mn + Ca), Py = 100 Mg/(Fe + Mg + Mn + Ca) and Gr = 100 Ca/(Fe + Mg + Mn + Ca). Some grains have narrow, comparatively grossular-rich rims (Alm_{45} $Spss_1Py_{24}Grs_{30}$). These rims are compositionally similar to garnet in the GRZ. Garnet forming part of structured coronas in the GRZ is zoned, with an increase in grossular content and a decrease in pyrope content from the inner towards the outer parts of the coronas. Garnet on the outermost parts of the coronas is $Alm_{44}Spss_1Py_{29}Gr_{26}$. Large garnet grains from low D4 strain domains in the Milford Gneiss are homogeneous grossular-rich almandine ($Alm_{50}Spss_2Py_{28}Gr_{20}$). D4 garnet from the adjacent high-strain domains is also homogeneous, but richer in grossular than garnet in the low-strain domains, having compositions that fall between Alm_{57} $Spss_1Py_{10}Gr_{22}$ and $Alm_{43}Spss_1Py_{24}Gr_{31}$. S4 garnet in the Milford Gneiss is compositionally similar to garnet in D3 and D4 mylonite zones that cut the Pembroke Granulite. Garnet in the Western Fiordland Orthogneiss has a restricted range in composition between $Alm_{43}Spss_1Py_{38}Grs_{18}$ and $Alm_{48}Spss_1Py_{32}Gr_{19}$.

Epidote group minerals include clinozoisite in S4 assemblages of the Milford Gneiss, and epidote in most rock types from the Anita Shear Zone. Ferric iron in epidote analyses was calculated assuming two-site ordering with a total of six silica, aluminium and ferric cations per 12.5 oxygens. Clinozoisite in S4 assemblages of the Milford Gneiss has Cz = (Al–2) $\approx$ 0.5–0.7. S1 *biotite* in the Pembroke Granulite has X_{Fe} 0.44–0.46 and comparatively high Ti content, with approximately 0.65 Ti per formula unit (pfu; 22 oxygens). Biotite in the Western Fiordland Orthogneiss at Poison Bay has X_{Fe} 0.30–0.38 and 0.21–0.45 Ti pfu.

Table 1. Representative microprobe analyses of some critical rock types.

	9635a—Garnet reaction zone			9637d—Garnet reaction zone			9606—Milford Gneiss S4						9641a—S4 mylonite				
	g	cpx	plag	g	cpx	plag	ky	cz	g	hb	pl	marg	g	cpx	hb	pl	bi
SiO_2	39.40	52.65	61.97	38.93	52.66	61.55	36.83	38.37	38.01	42.54	62.58	33.64	38.59	51.55	39.83	63.06	36.59
TiO_2	0.06	0.29	0.00	0.05	0.20	0.02	0.02	0.12	0.07	0.61	0.01	0.15	0.05	0.53	1.29	0.00	3.86
Al_2O_3	22.19	7.98	23.70	21.60	5.55	24.17	62.76	28.15	21.59	16.52	23.01	47.62	21.61	8.24	14.31	23.03	14.97
Cr_2O_3	0.00	0.00	0.04	0.00	0.01	0.01	0.00	0.00	0.00	0.03	0.00	0.08	0.00	0.00	0.00	0.00	0.00
FeO	19.13	4.20	0.04	21.35	6.57	0.02	0.53	6.51	25.94	12.91	0.03	0.78	22.34	6.98	15.78	0.18	14.09
MnO	0.22	0.00	0.00	0.49	0.03	0.02	0.02	0.02	2.24	0.18	0.00	0.02	2.08	0.10	0.11	0.00	0.06
MgO	7.84	11.90	0.00	8.08	11.91	0.00	0.00	0.00	4.74	11.17	0.00	0.31	4.94	9.82	9.37	0.00	13.98
CaO	11.21	19.70	4.98	9.52	19.55	5.22	0.02	23.31	6.96	10.48	4.22	8.92	10.38	18.64	11.28	4.16	0.06
Na_2O	0.03	2.90	8.47	0.00	2.64	8.36	0.00	0.00	0.01	1.98	9.20	2.60	0.02	3.30	1.58	9.22	0.05
K_2O	0.02	0.01	0.30	0.03	0.00	0.33	0.00	0.02	0.00	0.46	0.08	0.27	0.00	0.00	2.07	0.26	9.34
Total	100.09	99.62	99.50	100.03	99.13	99.79	100.17	96.49	99.56	96.88	99.14	94.39	100.01	99.16	95.60	99.90	93.00
Oxygen	12	6	8	12	6	8	5	13	12	23	8	22	12	6	23	8	22
Si	2.992	1.914	2.759	2.982	1.948	2.740	0.995	3.052	2.992	6.261	2.791	4.480	2.999	1.907	6.145	2.794	5.582
Ti	0.003	0.008	0.000	0.003	0.006	0.001	0.000	0.007	0.004	0.067	0.000	0.015	0.003	0.015	0.149	0.000	0.443
Al	1.986	0.342	1.244	1.950	0.242	1.266	1.998	2.640	2.004	2.866	1.210	7.477	1.980	0.359	2.602	1.203	2.692
Cr	0.000	0.000	0.001	0.000	0.000	0.000	0.000	0.000	0.000	0.003	0.000	0.008	0.000	0.000	0.000	0.000	0.000
Fe	1.215	0.128	0.002	1.368	0.203	0.001	0.012	0.433	1.708	1.589	0.001	0.087	1.452	0.216	2.036	0.007	1.797
Mn	0.014	0.000	0.000	0.032	0.001	0.001	0.000	0.001	0.149	0.023	0.000	0.002	0.137	0.003	0 014	0.000	0.008
Mg	0.888	0.645	0.000	0.923	0.657	0.000	0.000	0.000	0.556	2.449	0.000	0.062	0.572	0.542	2.155	0.000	3.180
Ca	0.912	0.768	0.238	0.781	0.774	0.248	0.001	1.987	0.587	1.653	0.202	1.273	0.864	0.739	1.864	0.197	0.010
Na	0.004	0.204	0.731	0.000	0.189	0.721	0.000	0.000	0.001	0.564	0.796	0.672	0.002	0.236	0.471	0.792	0.014
K	0.002	0.001	0.017	0.003	0.000	0.018	0.000	0.002	0.000	0.086	0.005	0.047	0.000	0.000	0.407	0.015	1.817
Total	8.015	4.009	4.992	8.041	4.020	4.996	3.006	8.122	8.002	15.562	5.004	14.122	8.009	4.017	15.844	5.008	15.544

S4 biotite in the Milford Gneiss has X_{Fe} 0.38–0.45 (0.1–0.18 Ti pfu). Phengitic *white mica* defines S4 in Milford Gneiss samples, apparently in textural equilibrium with the other minerals. It has approximately 6.3 Si cations per formula unit (22 oxygens), and approximately 15% paragonite content. *Margarite* in sample 9606 has approximately 30% paragonite content. *Scapolite* in GRZ has the composition $Me = (Ca + Mg + Fe + Mn + Ti)/(Na + K + Ca + Mg + Fe + Mn + Ti) = 0.66$. *Rutile* contains $<1\%$ ferric iron. *Ilmenite* contains $<2\%$ pyrophanite and $<4\%$ geikielite. *Kyanite* commonly contains 0.5–1% Fe^{3+}.

THERMOBAROMETRY

P–T estimates obtained from applying a variety of thermobarometric techniques to the mineral assemblages described above are summarized in Table 2. The earliest assemblages in the Arthur River Complex for which reliable *P–T* estimates can be made come from the garnet reaction zones. For sample 9635a, the compositions of adjacent garnet and clinopyroxene grains indicate $T \approx 800\,^{\circ}C$ for $P = 14$ kbar. In this discussion, all temperature estimates for garnet–clinopyroxene thermometry follow Ellis & Green (1979); estimates following the methods of Powell (1985) and Krogh (1988) are shown in Table 2. If a correction is made for aegirine content, the temperature estimate for sample 9635a drops to approximately 750 °C (Table 2). Assuming that $T = 750\,^{\circ}C$, the compositions of co-existing plagioclase, garnet, clinoproxene and quartz indicate that $P = 16.1$ or 14.2 kbar, from the methods of Eckert *et al.* (1991) and Newton & Perkins (1982), respectively.

The assemblage kyanite, garnet and plagioclase in sample 9606b (Milford Gneiss) gives the most precise estimates for conditions that accompanied the development of S4. The compositions of adjacent parts of S4 garnet and hornblende give $T \approx 670\,^{\circ}C$ (after Graham & Powell, 1984), and for $T = 700\,^{\circ}C$ the compositions of adjacent grains for the assemblage garnet, plagioclase, kyanite and quartz give $P = 13.2$ kbar (after Newton & Hasleton, 1981). *P–T* conditions may also be estimated using the average pressure–temperature (*PT*) method, using microprobe analyses of the minerals and the computer software, THERMOCALC (version 2.5; Powell & Holland, 1988), with the internally consistent thermodynamic dataset of Holland & Powell (1990; datafile created April 1996). All mineral end-member activities were calculated using the computer program AX (shareware written by T.J.B. Holland, http://www.esc.cam.ac.uk/software.html) and the defaults suggested in Powell & Holland (1988). Average pressure calculations for $T = 700\,^{\circ}C$ made for the S4 assemblage garnet, hornblende, plagioclase, biotite, clinozoisite, kyanite and quartz in sample 9606b indicate 15.8 ± 2.6 kbar (2 σ); average temperature calculations for $P = 16$ kbar returned $T = 702 \pm 104\,^{\circ}C$. The *P–T* results from the different methods are within the 2 σ estimated using THERMOCALC.

Sample 9608c is a coarse-grained recrystallized leucogabbro that contains the S4 assemblage garnet, clinopyroxene, plagioclase and quartz. Garnet–clinopyroxene thermobarometry returns estimates of $T \approx 900\,^{\circ}C$ that drop to $T \approx 800\,^{\circ}C$ when an aegirine correction is made to the diopside composition. For $T = 700\,^{\circ}C$, the composition of adjacent grains of S4 garnet, clinopyroxene, plagioclase and quartz give

Table 2. *P–T* estimates obtained from applying a variety of thermobarometric techniques to the mineral assemblages. Methods: (1) Ellis & Green (1979); (2) Powell (1985); (3) Krogh (1988); (4) Eckert *et al.* (1991); (5) Newton & Perkins (1982); (6) Graham & Powell (1984); (7) Newton & Haselton (1981); (8) Powell & Holland (1988).

Rock	Location (Milford 1:50 000 grid)	Assemblage	Timing	Assumed *P* (kbar)	*T* (°C)	Calculated result *T* (°C)	*P* (kbar)	Method
9637d	Above Stirling Falls	g–cpx–pl–q–ky	GRZ	14	all Fe^{2+}	871, 856, 852		1, 2, 3
	21024 56126				Fe^{3+} corrected	765, 747, 732		1, 2, 3
					750		15.6, 13.7	4, 5
					750		14.1	7
9635a1	W of Stirling Falls	g–cpx–pl–q	GRZ	14	all Fe^{2+}	812, 795, 788		1, 2, 3
	21018 56908				Fe^{3+} corrected	746, 728, 715		1, 2, 3
					750		16.1, 14.2	4, 5
9606b	W of Stirling Falls	g–hbl–pl–q–ky	S_4			674		6
	21029 56095				700		13.2	7
		g–hbl–pl–bi–ep–ky–q			700		15.8 ± 2.6	8
				16	702 ± 104			
9608c	W of Stirling Falls	g–cpx–hbl–pl–q	S_4	14	all			
Fe^{2+}	899, 886, 888		1, 2, 3					
	21016 56096				Fe^{3+} corrected	822, 806, 800		1, 2, 3
					700		13.6, 11.7	4, 5
					800		14.9, 12.9	4, 5
9636e2	above Stirling Falls	g–cpx–pl–q	S_4 def. GRZ	14	all Fe^{2+}	775, 757, 742		1, 2, 3
	21024 56126				Fe^{3+} corrected	669, 648, 624		1, 2, 3
					700	13.7, 11.8		4, 5
9646b	N shore Poison Bay	g–cpx–hbl–pl–q	S_4	14		820, 801, 768		1, 2, 3
	20872 55013				700		14.3, 12.4	4, 5
					800		15.6, 13.7	4, 5
9641a	Pembroke Valley	g–cpx–pl–q	S_4 mylonite	14		699, 679, 662		1, 2, 3
	21044 56120				697			6
					700		16.6, 14.7	4, 5
9653	WFO, Poison Bay	g–cpx–pl–q			750		12.6 ± 1.9	8
	20867 55996			12.6		718 ± 115		8

$P = 13.6$ and 11.7 kbar, after Eckert *et al.* (1991) and Newton & Perkins (1982), respectively. Sample 9636e is taken from a GRZ in the Milford Gneiss that underwent recrystallization during D4, such that granoblastic garnet, clinopyroxene, quartz and plagioclase define S4. Assuming $P = 14$ kbar, garnet–clinopyroxene thermometry returns $T = 775\,^{\circ}C$ or $670\,^{\circ}C$ (aegirine correction). Assuming $T = 700\,^{\circ}C$, the composition of S_4 garnet, clinopyroxene, plagioclase and quartz return $P = 13.7$ or 11.8 kbar, after Eckert *et al.* (1991) and Newton & Perkins (1982), respectively. A sample of the Milford Gneiss taken from a zone of comparatively low strain in the Jagged Gneiss along the north shore of Poison Bay contains the S4 assemblage garnet, clinopyroxene, hornblende and quartz (9646b) and gives *P–T* estimates that are within error of those from Milford Sound (Table 2).

Sample 9641a is taken from a D4 mylonite that cuts the Pembroke Granulite and includes the S4 assemblage garnet, hornblende, clinopyroxene, plagioclase and quartz. Garnet–clinopyroxene thermometry gives $T = 700\,^{\circ}C$, consistent with $T = 697\,^{\circ}C$ from garnet–hornblende thermometry (Graham & Powell, 1984; Table 2). For $T = 700\,^{\circ}C$, the compositions of adjacent grains of garnet, clinopyroxene and plagioclase give $P = 16.6$ or 14.7 kbar (Eckert *et al.*, 1991 and Newton & Perkins, 1982; respectively).

P–X_{H_2O} pseudosection

The thermobarometric results are useful for the purpose of inferring conditions that accompanied the formation of low-variance assemblages. However, the available techniques do not indicate, for example, the pressure conditions that accompanied formation of the S1 assemblage in the Pembroke Granulite. In addition, they give little information with respect to the proportion of fluid that accompanied the development of the GRZ assemblages compared with that in the S4 assemblages. *P–T* pseudosections, calculated with H_2O in excess, are suitable where H_2O-saturated conditions can be inferred, but inappropriate for examining mineralogical changes that involved water-undersaturated conditions, as inferred, for example, in the formation of the GRZ.

To examine these changes in conditions, a quantitative *P–*X_{H_2O} pseudosection has been constructed in the model system CNFMASH ($CaO–Na_2O–FeO–MgO–Al_2O_3–SiO_2–H_2O$), using THERMOCALC (version 2.6) and the '20 April 1996' internally consistent thermodynamic dataset (Powell *et al.*, 1998). Details of the use of THERMOCALC for grid and pseudosection construction are outlined in Powell *et al.* (1998). Minerals included in the construction of the grid are garnet (g), hornblende (hb), clinozoisite (cz), kyanite (ky), orthopyroxene (opx), clinopyroxene (cpx), plagioclase and quartz. Most of the activity models used in the calculations assume ideal mixing on all sites and are identical to those used by Powell *et al.* (1998), with the exception of hornblende. We used the hornblende activity model presented by Carson *et al.* (1999) to construct the diagram. Where present, the fluid phase is assumed to be pure H_2O. In the *P–*X_{H_2O} diagram, H_2O is considered explicitly

(Guiraud *et al.*, 1996; Carson *et al.*, 1999): X_{H_2O} is defined as the molar proportion of the component, H_2O, in the bulk composition. Fig. 5(a) represents a P–X_{H_2O} pseudosection appropriate to the gabbroic gneiss that forms most of the Pembroke Granulite. On the basis of the thermobarometry outlined above, it is drawn at fixed $T = 750\,^{\circ}C$ for $P = 4$–20 kbar. The rock composition used was obtained from XRF whole-rock analyses, and varies (Fig. 5) from $Al_2O_3 = 26.8$, $CaO = 24.5$, $MgO = 21.2$, $FeO = 17.3$, $Na_2O = 10.2$, $H_2O = 0.0$ ($X_{H_2O} = 0$) to $Al_2O_3 = 25.03$, $CaO = 22.9$, $MgO = 19.8$, $FeO = 16.2$, $Na_2O = 9.6$, $H_2O = 6.5$ ($X_{H_2O} = 0.13$). The

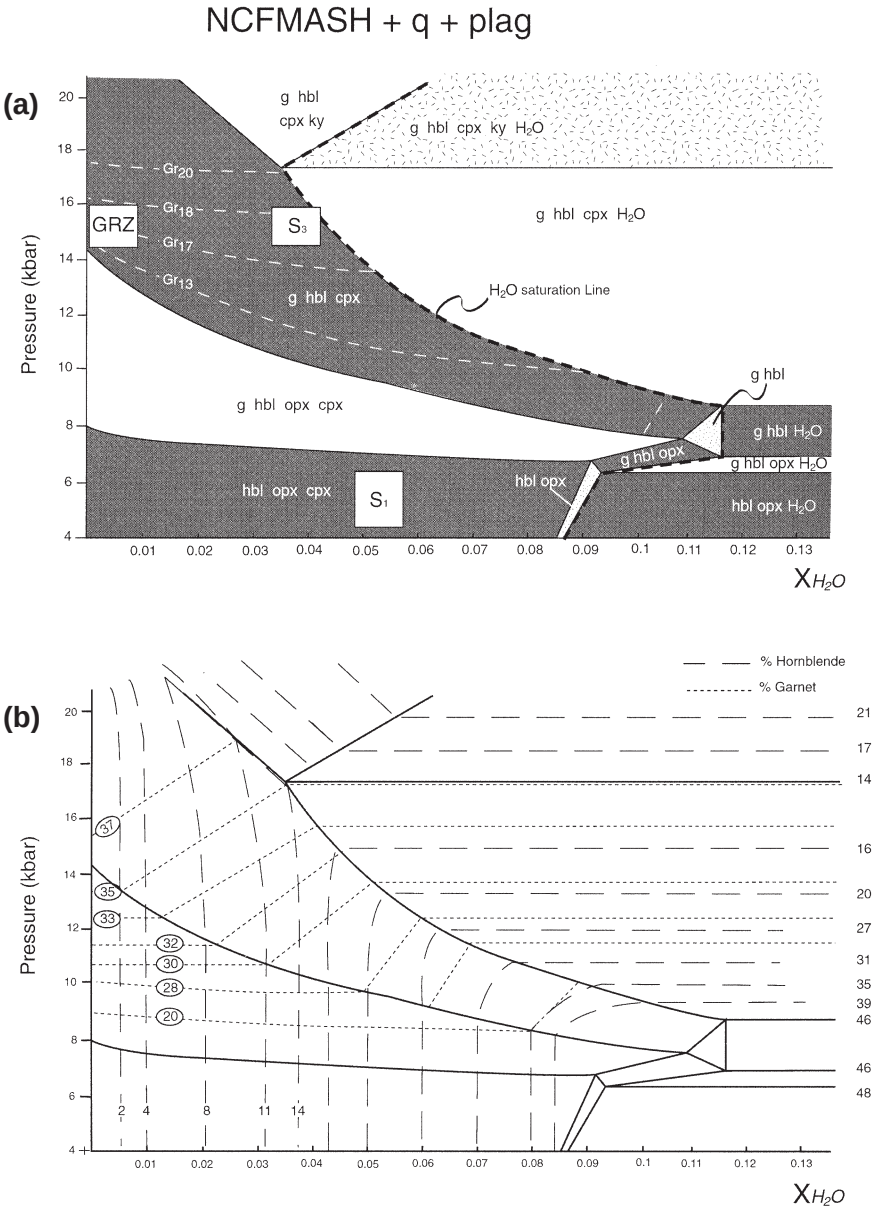

Fig. 5. (a) P–X_{H_2O} pseudosection for $T = 750\,^{\circ}C$ and $P = 4$–20 kbar, constructed in the system CaO–Na_2O–FeO–MgO–Al_2O_3–SiO_2–H_2O using THERMOCALC (version 2.6) and the '20 April 1996' internally consistent thermodynamic dataset (Powell *et al.*, 1998) from $Al_2O_3 = 26.8$, $CaO = 24.5$, $MgO = 21.2$, $FeO = 17.3$, $Na_2O = 10.2$, $H_2O = 0.0$ ($X_{H_2O} = 0$) to $Al_2O_3 = 25.03$, $CaO = 22.9$, $MgO = 19.8$, $FeO = 16.2$, $Na_2O = 9.6$, $H_2O = 6.5$ ($X_{H_2O} = 0.13$). These rock compositions match XRF whole-rock analyses of gabbroic gneiss in the Pembroke Granulite. The pseudosection is drawn for quartz and plagioclase in excess. Minerals included in the construction of the grid were garnet (g), hornblende (hb), clinozoisite, kyanite (ky), orthopyroxene (opx), clinopyroxene (cpx), plagioclase and quartz. Most activity models assume ideal mixing on sites and are identical to those used in Powell *et al.* (1998), although the hornblende model presented in Carson *et al.* (1999) was used for this diagram. Where present, the fluid phase is assumed to be pure H_2O. X_{H_2O} is defined as the molar proportion of the component, H_2O, in the bulk composition, and the addition or subtraction of H_2O at a given P is represented by a horizontal line on the diagram. The dashed white lines in the quadrivariant field garnet–hornblende–clinopyroxene–plagioclase–quartz indicate the isopleths of grossular content in garnet. (b) Part (a) contoured for modal hornblende and garnet.

pseudosection is drawn for quartz and plagioclase in excess, and illustrates the mineral evolution with respect to changing pressure and X_{H_2O}, as well as the preservation of various mineral assemblages in terms of recrystallization and fluid availability. The addition or subtraction of H_2O at a given pressure is represented by a horizontal line on the diagram. The indicated H_2O saturation line (Fig. 5a) is the limiting boundary beyond which any further increase of X_{H_2O} mainly increases the mode of fluid. Figure 5(a) illustrates the change in metabasic assemblages from those at low-P involving hornblende, orthopyroxene, clinopyroxene and plagioclase, through assemblages involving garnet, clinopyroxene, hornblende and plagioclase with or without orthopyroxene at intermediate-P conditions, to assemblages involving garnet, clinopyroxene, plagioclase and kyanite at high-P conditions. A limitation of the diagram at high-P is the absence of omphacite from the datafile (e.g. Holland & Powell, 1998), but as the maximum pressure conditions experienced by the Pembroke Granulites involved $P \approx 16$ kbar at elevated conditions and omphacite has not been reported from Fiordland, this does not present a serious limitation to the application of the diagram here.

Errors on univariant lines in the pseudosection are mostly a product of errors on the enthalpy data used in the Holland & Powell (1990) dataset. The 2 σ error on the position of the upper boundary of the quadrivariant field involving orthopyroxene, clinopyroxene and hornblende is 0.4 kbar for $T = 750\,^{\circ}C$. Increasing the inferred temperature conditions to $T = 800\,^{\circ}C$ moves the univariant curve to pressure conditions approximately 0.5 kbar higher than at $T = 750\,^{\circ}C$ (Fig. 5a). The 2 σ error on the position of the univariant curve defining the upper pressure limit of orthopyroxene at water-undersaturated conditions is also 0.4 kbar for $T = 750\,^{\circ}C$. Increasing the inferred temperature conditions to $T = 800\,^{\circ}C$ has the effect of moving this univariant curve 1.2 kbar higher at $X_{H_2O} = 0.01$, reducing to 0.5 kbar higher at $X_{H_2O} = 0.08$. The position of the water saturation boundary defining the upper pressure limit of the quadrivariant field involving garnet, hornblende and clinopyroxene is less precisely defined. The 2 σ error on this univariant at $T = 750\,^{\circ}C$ and $X_{H_2O} = 0.04$ is 3.4 kbar, reducing to 2.2 kbar for $X_{H_2O} = 0.08$. This univariant is also quite sensitive to changes in temperature: increasing the inferred temperature conditions to $T = 800\,^{\circ}C$ has the effect of lowering estimated pressures by 1.5 kbar at $X_{H_2O} = 0.04$ and 1.0 kbar at $X_{H_2O} = 0.08$. The major effect of increasing the estimated temperature is to shrink the pressure range of the quadrivariant field involving garnet, hornblende and clinopyroxene.

Major changes in the mineralogy of the Pembroke Granulite between D1 and D3 mostly involved the consumption of hornblende and growth of garnet and clinopyroxene. To constrain the position of the S1 assemblage of the Pembroke Granulite in the hornblende–orthopyroxene–clinopyroxene quadrivariant field, Fig. 5(b) shows the various fields contoured for modal hornblende and garnet. The absence of garnet indicates that conditions that accompanied the development of S1 involved $P < 7.5$ kbar. The modal abundance of hornblende constrains $X_{H_2O} \approx 0.05$ (Fig. 5a). In domains of low D1 strain, higher proportions of igneous orthopyroxene persist and it seems reasonable to assume that the igneous protolith crystallized at lower X_{H_2O} but similar pressure conditions to those that accompanied D1. The interpretation that igneous protoliths to the Arthur River Complex crystallized in the mid- to upper crust is confirmed by two-pyroxene igneous assemblages (Fig. 5a) and rare olivine–plagioclase-bearing gabbros, which are restricted to $P < 8$ kbar for common tholeiitic compositions (Green & Ringwood, 1967). Mineral assemblages in the GRZ involve the growth of garnet and clinopyroxene at the expense of S1 hornblende and plagioclase. In the cores of the garnet reaction zones, the near complete consumption of S1 hornblende is consistent with conditions having involved very low X_{H_2O}. There were probably centimetre-scale variations in X_{H_2O} in the garnet reaction zones, as the proportion of hornblende decreases and the proportion of clinopyroxene increases as the core of the GRZ is approached. Thus, the GRZ zone assemblage is unlikely to reflect the trivariant assemblage garnet, hornblende, clinopyroxene and H_2O. Water activity was probably less than 1, and the intersection of appropriate garnet and hornblende isopleths places the GRZ assemblage in the quadrivariant assemblage garnet, hornblende and clinopyroxene at $X_{H_2O} \approx 0.01$ and $P \approx 15$ kbar (Fig. 5b). This is in good agreement with the results from thermobarometry presented above. In D3 shear zones that cut garnet reaction zones, the recrystallization of corona reaction textures resulted in grain size coarsening but little modal change compared with garnet reaction zones outside the shear zones. We infer that conditions that accompanied the development of S3 were similar to those that accompanied the formation of the garnet reaction zones. Mylonites that define S4 have more hornblende and less garnet and clinopyroxene than either the GRZ or S3 assemblages. The intersection of appropriate hornblende and garnet isopleths for S4 mylonite assemblages in the Pembroke Valley is consistent with conditions close to the water saturation line at $X_{H_2O} \approx 0.04$ and $P \approx 15$ kbar (Fig. 5b). Slightly higher modal hornblende present in similar S4 assemblages of the Milford Gneiss could reflect water-saturated conditions.

The recrystallization of GRZ assemblages to S4 assemblages reflects increased water activity. However, X_{H_2O} conditions inferred for the S4 assemblages are similar to those inferred for S4 assemblages (Fig. 5a); so the localized recrystallization simply consumed fluid available in S1 hornblende. There was limited recrystallization of the low-P S1 assemblages in the Pembroke Granulite to the high-P GRZ S3 or S4 assemblages. The spatial density of the garnet reaction

zones varies considerably, but overall they collectively occupy $<20\%$ of the surface area of the Pembroke Granulites. It seems reasonable to assume that rocks outside the garnet reaction zones, or D3 or D4 mylonites, were at P–T conditions close to, if not identical to, the areas that experienced recrystallization. That S1 assemblages metastably persisted through the sequence of high-P events most probably reflects conditions of low strain intensity. Similar features have been documented where eclogite facies shear zones cut anorthosite in the Bergen Arcs (e.g. Griffin, 1972) or dolerite in central Australia (White & Clarke, 1997). The negative slope of the water saturation surface on the P–X_{H_2O} diagram is consistent with the increase in pressure from conditions that accompanied the development of S1 to those that accompanied the development of S4 having enabled fluid-undersaturated rocks to become fluid-saturated—if they were deformed during D4. Once liberated, fluid could have assisted further recrystallization as we infer for the change from S1 assemblages in the Pembroke Granulite to the enveloping S4 assemblages in the Milford Gneiss.

Within the quadrivariant assemblage garnet, hornblende and clinopyroxene, isopleths of grossular content of garnet have shallow negative slopes close to the low-P boundary of the field (Fig. 5b). Grossular content is predicted by us to increase from approximately Grs_{10} along the low-P boundary, to Grs_{21} at the low-P end of the trivariant assemblage garnet, hornblende, clinopyroxene and kyanite (Fig. 5a). The predicted grossular content for the position of GRZ indicated on Fig. 5(a) would be approximately Gr_{18}. The observation of large, unzoned garnet grains in post-S1 igneous veins is consistent with a marked pressure increase (relative to the conditions that accompanied D1) having preceded their emplacement. These garnet grains, and garnet in low-strain S4 assemblages of the Milford Gneiss, have compositions of $Gr_{16–20}$, and are cut by high-strain S4 assemblages containing garnet with $Gr_{22–30}$. This change is poorly constrained from the viewpoint of any influence of bulk-rock geochemistry. However, the lower ranges of the grossular content in the natural assemblages agree reasonably well with the model system, and the refinement of mixing models for garnet is currently on-going (Holland & Powell, 1998). The systematic change in grossular content is consistent with the water-saturated S4 assemblages having developed during continued burial of the terrane, D4 having accompanied an increase in pressure conditions of 2–4 kbar. The garnet-bearing post-S_1 igneous veins and garnet reaction zones constrain the major increase in pressure (of approximately 8 kbar) to have preceded D4.

DISCUSSION

Rocks of the Arthur River Complex experienced polyphase granulite facies metamorphism and deformation at mid- to lower crustal levels that variably recrystallized gabbros and diorites. The earliest metamorphic event formed two pyroxene–hornblende gneisses of the Pembroke Granulite and occurred at conditions of $P<7.5$ kbar, possibly soon after the emplacement of igneous protoliths. The Arthur River Complex then experienced an increase in pressure of the order of $P=8$ kbar some time between the development of S1 and the formation of the garnet reaction zones. Large, homogeneous garnet grains in leucogabbroic and dioritic igneous veins that cut S1 but are, in turn, cut by the garnet reaction zones most probably reflect vein emplacement under comparatively high-P conditions. Although less well constrained from the viewpoint of bulk rock composition, the Early Cretaceous Western Fiordland Orthogneiss was emplaced at mid-crustal levels, *before* an increase in pressure that resulted in garnet–clinopyroxene corona reaction textures on igneous orthopyroxene. Effects of this increase in pressure are also preserved in jadeite zoning in clinopyroxene grains from parts of the Western Fiordland Orthogneiss (Bradshaw, 1989a). Garnet reaction zones similar to those described above for the Arthur River Complex have been reported from parts of the Fiordland Complex as far south as Doubtful Sound (Oliver, 1980), including parts of the Western Fiordland Orthogneiss (Bradshaw, 1989b). The origin of the veins is not discussed here, but they are sufficiently unusual that it is unlikely that there were two vein-forming events. As they occur within the Western Fiordland Orthogneiss, they are younger than 119 Ma and indicate that the regional high-P metamorphic assemblages that formed in the Milford and Harrison Gneiss are Cretaceous. The effects of penetrative D4 deformation extend some 10 km westward from the Darran Complex to where S4 is cut by the Anita Shear Zone (Fig. 2). These Cretaceous high-P assemblages occur regionally: more than 15 km distal, and unrelated, to the Western Fiordland Orthogneiss (Fig. 2). Hence, heating during emplacement of the Western Fiordland Orthogneiss cannot have been the sole cause of the Cretaceous metamorphism.

The contact between the Arthur River Complex and the late Jurassic/early Cretaceous Darran Complex (Blattner, 1991; part of the Median Tectonic Zone) at Milford Sound reflects a strain and metamorphic gradient (Blattner, 1991; Hollis, 1996), although the boundary is faulted further north (Blattner, 1991) and south (Bradshaw, 1990). In most interpretations, the contact represents the western limit of the Median Tectonic Zone, and the Arthur River Complex is placed within the Western Province of New Zealand (e.g. Kimbrough *et al.*, 1994). However, amphibolite facies Palaeozoic schists that characterize the Western Province in western Fiordland mostly escaped the thermally perturbed Early Cretaceous conditions recorded by rocks of the Arthur River Complex, Western Fiordland Orthogneiss and Median Tectonic

Zone. The stitching of Median Tectonic Zone rocks to the Western Province is indicated by granites of the *c*. 126–105 Ma Separation Point Suite (Kimbrough *et al*., 1994), which is inferred to be the higher-level equivalent of the Western Fiordland Orthogneiss (e.g. Muir *et al*., 1998). Muir *et al*. (1998) suggested that the comparatively sudden appearance of this extensive Early Cretaceous magmatism was related to the thrusting of parts of the Median Tectonic Zone, such as the Darran Complex, beneath Western Province rocks. Major and trace element patterns, Sr and oxygen isotope ratios are consistent with the Pembroke Granulite and Milford Gneiss being, at least in part, the equivalents of the Darran Complex (Blattner, 1991), deformed and metamorphosed in the Early Cretaceous. Irrespective of whether the Arthur River Complex is part of the Median Tectonic Zone or the Western Province, it experienced Early Cretaceous burial (Mattinson *et al*., 1986; Bradshaw, 1989a). This result contrasts with the interpretation of Gibson & Ireland (1995) that the Mesozoic history of western Fiordland rocks involved only decompression. The emplacement of the Western Fiordland Orthogneiss occurred at mid-crustal conditions and preceded early Cretaceous deformation and a pressure increase equivalent to burying the terrane approximately 25 km deeper in the crust. On the basis of these interpretations, the burial and high-*P* metamorphism of the Arthur River Complex were a consequence of collision and not magmatic over-accretion (cf. Brown, 1996). We prefer an interpretation involving the Arthur River Complex being the deformed root of a magmatic arc, part of the Median Tectonic Zone, which was thrust under the Pacific Gondwana margin, now represented by Western Province rocks. We infer that convergence-related Early Cretaceous deformation accompanied burial and outlasted magmatism in western Fiordland.

CONCLUSIONS

Igneous protoliths of both the Arthur River Complex and Western Fiordland Orthogneiss were emplaced in the mid-crust, before being tectonically buried in the Early Cretaceous to lower crustal conditions. The high-*T*, high-*P* granulite facies conditions involving $T > 750\,^{\circ}\mathrm{C}$ and $P \approx 14$ kbar were produced in a convergent margin setting, which involved the collision and accretion of Jurassic to Early Cretaceous arc material to the Gondwana Pacific margin. Early Cretaceous convergent deformation outlasted magmatism and induced burial of the Arthur River Complex and Western Fiordland Orthogneiss.

ACKNOWLEDGEMENTS

Funding to support this work was provided by the Australian Research Council (ARC grant A10009053 to G.L.C. and K.A.K., and University of Sydney Institutional grants to K.A.K.). N.R.D. was supported by an Australian Postgraduate Award from the University of Sydney. We thank the Department of Land Conservation in Te Anau for permission to visit and sample localities in the Fiordland National Park, and J. Hill, N. Mortimer and A. Tulloch for helpful discussions. Fieldwork started when G.L.C. was a visitor at the Department of Geology, University of Canterbury, New Zealand; S. Weaver and D. Shelley are thanked for their support. Thanks also go to R.W. White, T. Patrick, J. Hollis, H. Degeling and L. Turner for their enthusiastic assistance in the field. Critical reviews by E.H. Brown, A.F. Cooper, A.J. Tulloch and R.W. White and the careful editorial work of R.H. Vernon considerably improved an earlier version of the manuscript.

REFERENCES

Austrheim, H. & Griffin, W. L., 1985. Shear deformation and eclogite formation within granulite-facies anorthosites of the Bergen Arcs, western Norway. *Chemical Geology*, **50,** 267–281.

Bishop, D. G., Bradshaw, J. D. & Landis, C. A., 1985. Provisional terrain map of South Island, New Zealand. In: *Tectonostratigraphic Terranes of the Circum-Pacific Region* (eds Howell, D. G., Jones, D. L., Cox, A. & Nur, A.), pp. 512–522, Circum-Pacific Council for Energy and Resources, Houston, Texas.

Blattner, P., 1976. Replacement of hornblende by garnet in granulite facies assemblages near Milford Sound, New Zealand. *Contributions to Mineralogy and Petrology*, **55,** 181–190.

Blattner, P., 1991. The North Fiordland transcurrent convergence. *New Zealand Journal of Geology and Geophysics*, **34,** 553–542.

Blattner, P. & Black, P. M., 1980. Apatite and scapolite as petrogenetic indicators in granolites of Milford Sound, New Zealand. *Contributions to Mineralogy and Petrology*, **74,** 339–348.

Bradshaw, J. Y., 1985. Geology of the northern Franklin Mountains, northern Fiordland, New Zealand, with emphasis on the origin and evolution of Fiordland granulites. *PhD Thesis, University of Otago, Dunedin, New Zealand.*

Bradshaw, J. Y., 1989a. Origin and metamorphic history of an Early Cretaceous polybaric granulite terrain, Fiordland, southwest New Zealand. *Contributions to Mineral Petrology*, **103,** 346–360.

Bradshaw, J. Y., 1989b. Early Cretaceous vein-related garnet granulite in Fiordland, southwest New Zealand: a case for infiltration of mantle-derived CO_2-rich fluids. *Journal of Geology*, **97,** 697–717.

Bradshaw, J. Y., 1990. Geology of crystalline rocks of northern Fiordland: details of the granulite facies Western Fiordland Orthogneiss and associated rock units. *New Zealand Journal of Geology and Geophysics*, **33,** 465–484.

Brown, E. H., 1996. High-pressure metamorphism caused by magma loading in Fiordland, New Zealand. *Journal of Metamorphic Geology*, **14,** 441–452.

Carson, C. J., Powell, R. & Clarke, G. L., 1999. Calculated mineral equilibria for the eclogite facies in Na_2O–CaO–MgO–FeO–Al_2O_3–SiO_2–H_2O: application to the Pouébo Terrane, Pam Peninsula, New Caledonia. *Journal of Metamorphic Geology*, **18,** 79–90.

Carter, R. M., Landis, C. A., Norris, R. J. & Bishop, D. G., 1974. Suggestions towards a high-level nomenclature for New Zealand rocks. *Journal of the Royal Society of New Zealand*, **4,** 5–18.

Cawthorn, A. F. & Collerson, K. D., 1974. The recalculation of pyroxene endmember parameters and estimation of ferrous

and ferric iron content from microprobe analyses. *American Mineralogist*, **59,** 1203–1208.

Clarke, G. L. & Powell, R., 1991b. Decompressional corona and symplectite textures in granulites of the Musgrave Complex, central Australia. *Journal of Metamorphic Geology*, **9,** 441–450.

Daczko, N. R., 1997. Fabric development and finite strain patterns in a deep crustal shear zone, Northwest Fiordland, New Zealand. *Unpublished BSc (Honours) Thesis, University of Sydney, Sydney, Australia.*

Eckert, J. O., Newton, R. C. & Kleppa, O. J., 1991. The ΔH of reaction and recalibration of garnet–pyroxene–plagioclase–quartz geobarometers in the CMAS system by solution calorimetry. *American Mineralogist*, **76,** 148–160.

Ellis, D. J. & Green, D. H., 1979. An experimental study of the effect of Ca upon garnet–clinopyroxene Fe–Mg exchange equilibria. *Contributions to Mineralogy and Petrology*, **71,** 13–22.

Gibson, G. M., 1990. Uplift and exhumation of middle and lower crustal rocks in an extensional tectonic setting, Fiordland, New Zealand. In: *Exposed Cross-Sections of the Continental Crust* (ed. Salisbury, M. H. & Fountain, D. M.). Kluwer Academic Publishers, 71–101.

Gibson, G. M. & Ireland, T. R., 1995. Granulite formation during continental extension in Fiordland. *Nature*, **375,** 479–482.

Gibson, G. M., McDougall, I. & Ireland, T. R., 1988. Age constraints on metamorphism and the development of a metamorphic core complex in Fiordland, southern New Zealand. *Geology*, **16,** 405–408.

Graham, C. M. & Powell, R., 1984. A garnet–hornblende geothermometer; calibration, testing, and application to the Pelona Schist, Southern California. *Journal of Metamorphic Geology*, **2,** 13–31.

Green, D. H. & Ringwood, A. E., 1967. An experimental investigation of the gabbro to eclogite transformation and its petrologic application. *Geochimica et Cosmochimica Acta*, **3,** 767–834.

Greenfield, J. E., Clarke, G. L. & White, R. W., 1998. A sequence of partial melting reactions at Mt Stafford, central Australia. *Journal of Metamorphic Geology*, **16,** 363–378.

Griffin, W. L., 1972. Formation of eclogites and the coronas in anorthosites, Bergen Arcs, Norway. *Geological Society of America Memoir*, **135,** 37–62.

Guiraud, M., Powell, R. & Cottin, J.-Y., 1996. Hydration of orthopyroxene–cordierite-bearing assemblages at Laouni, Central Hoggar, Algeria. *Journal of Metamorphic Geology*, **14,** 467–476.

Harley, S. L., 1989. The origins of granulites: a metamorphic perspective. *Geological Magazine*, **126,** 215–247.

Hill, E. J., 1995a. The Anita Shear Zone: a major, middle Cretaceous tectonic boundary in northwestern Fiordland. *New Zealand Journal of Geology and Geophysics*, **38,** 93–103.

Hill, E. J., 1995b. A deep crustal shear zone exposed in western Fiordland, New Zealand. *Tectonics*, **14,** 1172–1181.

Holland, T. J. B. & Powell, R., 1990. An enlarged and updated internally consistent dataset with uncertainties and correlations: the system K_2O–Na_2O–CaO–MgO–MnO–FeO–Fe_2O_3–Al_2O_3–TiO_2–SiO_2–C–H_2–O_2. *Journal of Metamorphic Geology*, **8,** 89–124.

Holland, T. J. B. & Powell, R., 1998. An internally consistent thermodynamic dataset for phases of petrological interest. *Journal of Metamorphic Geology*, **16,** 309–343.

Hollis, J. A., 1996. The pressure–temperature history of Cretaceous granulites in Milford Sound, New Zealand. *Unpublished BSc (Honours) Thesis, University of Sydney, Sydney, Australia.*

Ireland, T. R. & Gibson, G. M., 1998. SHRIMP monazite and zircon geochronology of high-grade metamorphism in New Zealand. *Journal of Metamorphic Geology*, **16,** 149–167.

Kimbrough, D. L., Tulloch, A. J., Geary, E., Coombs, D. S. & Landis, C. A., 1993. Isotopic ages from the Nelson region of South Island, New Zealand; crustal structure and the definition of the Median Tectonic Zone. *Tectonophysics*, **225,** 443–448.

Kimbrough, D. L., Tulloch, A. J., Coombs, D. S., Landis, C. A., Johnston, M. R. & Mattinson, J. M., 1994. Uranium–lead zircon ages from the Median Tectonic Zone, New Zealand. *New Zealand Journal of Geology and Geophysics*, **37,** 393–419.

Klepeis, K. A., Daczko, N. & Clarke, G. L., 1999. Kinematic vorticity and the tectonic significance of superposed mylonites in a major lower crustal shear zone, northern Fiordland, New Zealand. *Journal of Structural Geology*, **21,** 1385–1405.

Koons, P. O., 1978. *Aspects of the geology of the southern Darran Mountains. New Zealand Geological Survey Report G26.* Unpublished report. Institute of Geological and Nuclear Sciences, Dunedin, New Zealand.

Krogh, E. J., 1988. The garnet–clinopyroxene Fe–Mg geothermometer: a reinterpretation of existing experimental data. *Contributions to Mineralogy and Petrology*, **99,** 44–48.

Leake, B. E., 1978. Nomenclature of amphiboles. *Mineralogical Magazine*, **42,** 533–563.

McLelland, J. M. & Whitney, P. R., 1977. The origin of garnet in the anorthosite–charnockite suite of the Adirondacks. *Contributions to Mineralogy and Petrology*, **60,** 161–181.

Mattinson, J. L., Kimbrough, D. L. & Bradshaw, J. Y., 1986. Western Fiordland orthogneiss: Early Cretaceous arc magmatism and granulite facies metamorphism, New Zealand. *Contributions to Mineralogy and Petrology*, **92,** 383–392.

Mortimer, N., 1995. Triassic to Early Cretaceous tectonic evolution of New Zealand terranes: a summary of recent data and an integrated model. In: *Proceedings of the 1995 PACRIM Congress* (eds Mauk, J. L. & St George, J. D.), pp. 401–406. Australasian Institute of Mining and Metallurgy, Carlton, Victoria, Australia.

Mortimer, N., Tulloch, A. J., Spark, R., Walker, N., Ladley, E., Kimbrough, D. L. & Allibone, A. H., 1999. Median Batholith and Median Suite of New Zealand: new perspectives on the Phanerozoic igneous record of southern Gondwanaland. *African Journal of Earth Sciences*, **29,** 257–268.

Muir, R. J., Ireland, T. R., Weaver, S. D., Bradshaw, S. D., Evans, J. A., Eby, G. N. & Shelley, D., 1998. Geochronology and geochemistry of a Mesozoic magmatic arc system, Fiordland, New Zealand. *Journal of the Geological Society of London*, **155,** 1037–1053.

Newton, R. C. & Hasleton, H. T., 1981. Thermodynamics of the garnet–plagioclase–Al_2SiO_5–quartz geobarometer. In: *Advances in Physical Geochemistry, Vol. 1* (eds Newton, R. C., Navrotsky, A. & Woods, B. J.), pp. 131–147. Springer Verlag, New York.

Newton, R. C. & Perkins, D., 1982. Thermodynamic calibration of geobarometers based on the assemblages garnet–plagioclase–orthopyroxene–clinopyroxene)–quartz. *American Mineralogist*, **67,** 203–222.

Oliver, G. J. H., 1980. Geology of the granulite and amphibolite facies gneisses of Doubtful Sound, Fiordland, New Zealand. *New Zealand Journal of Geology and Geophysics*, **1,** 27–41.

Powell, R., 1985. Regression diagnostics and robust regression in geothermometer/geobarometer calibration; the garnet–clinopyroxene geothermometer revisited. *Journal of Metamorphic Geology*, **3,** 231–243.

Powell, R. & Holland, T. J. B., 1988. An internally consistent dataset with uncertainties and correlations: 3. Applications to geobarometry, worked examples and a computer program. *Journal of Metamorphic Geology*, **6,** 173–204.

Powell, R., Holland, T. J. B. & Worley, B., 1998. Calculating phase diagrams with Thermocalc: methods and examples. *Journal of Metamorphic Geology*, **16**, 575–586.

Turner, R. L., 1998. Strain patterns and recrystallization in the lower crust; evidence from garnet reaction zones Fiordland, New Zealand. *Unpublished BSc (Honours) Thesis, University of Sydney, Sydney, Australia.*

White, R. W. & Clarke, G. L., 1997. The role of deformation in aiding recrystallization: an example from a high pressure shear zone. *Journal of Petrology*, **38,** 1307–1329.

Williams, J. G. & Harper, C. T., 1978. Age and status of the Mackay Intrusives in the Eglinton–Upper Hollyford area. *New Zealand Journal of Geology and Geophysics*, **21,** 733–742.

Wood, B. L., 1962. *New Zealand Geological Survey Map 1:250 000, Sheet 22, Wakatipu*. 1st edn. Institute of Geological and Nuclear Sciences, Wellington, New Zealand.

Wood, B. L., 1972. Metamorphosed ultramafites and associated formations near Milford Sound, New Zealand. *New Zealand Journal of Geology and Geophysics*, **15,** 88–127.

Received 21 December 1998; revision accepted 15 November 1999.